J Electr Eng Technol.2015; 10(3): 1154-1161
http://dx.doi.org/10.5370/JEET.2015.10.3.1154

ISSN(Print) 1975-0102
ISSN(Online) 2093-7423

Semi-lumped Balun Transformer using Coupled LC Resonators

Jongcheol Park*, Minkyu Yoon* and Jae Yeong Park†

Abstract – This paper presents a semi-lumped balun transformer using conventional PCB process and its design theory and geometry for the maximally flat response and wide bandwidth using magnetically coupled LC resonators. The proposed balun is comprised of two pairs of coupled resonators which share one among three LC resonators. It provides an identical magnitude and phase difference of 180° between two balanced ports with DC isolation and an impedance transformation characteristic. Theoretical design and analysis were performed to optimize the inductance and capacitance values of proposed balun device for obtaining the wide bandwidth and maximally flat response in its pass-band. Three balun transformers with a center frequency of 500 MHz were demonstrated for proving the concept of design proposed. They were fabricated by using lumped chip capacitors and planar inductors embedded into a conventional 4-layered PCB substrate. They exhibited a maximum magnitude difference of 0.8 dB and phase difference within 2.4 degrees.

Keywords: Baluns, Coupled circuits, Passives devices, Transformers, Resonators

1. Introduction

A balun (balanced-to-unbalanced) transformer is a transformer which converts balanced signals to unbalanced signals and vice versa. Many RF circuit modules and systems adopt a balanced input and output in order to improve the dynamic range by reducing the noise and even order harmonics [1-6]. As these RF modules and systems advance to be become smaller, lighter, and multi-functional with better performance, they generate a strong need for compact sized wideband balun devices [3-5, 7-17].

A large number of baluns devices have been reported to meet these requirements. The distributed-type balun device, especially the Marchand balun design [1], is the most popular one. It is applied to low temperature co-fired ceramics, multi-layered ceramics, and microwave integrated circuit chips and modules because it has a simple structure, sufficiently large bandwidth, and a reasonable phase difference and power distribution [7-9, 11, 13, 14, 16-18]. These modified Marchand balun consists of four quarter-wave length coupled lines which are implemented as a meander-shaped line [8, 14] or spiral-shaped line for miniaturization [7, 9, 16]. The LC resonance and stepped impedance methods were also proposed to reduce the physical length of the utilized coupled line [11, 13]. Moreover, a novel approach for miniaturization of the distributed-type balun was also introduced by using three quarter-wave length coupled lines [17, 18]. Whilst these various distributed-type baluns have been studied intensively for miniaturization, they still have some limitations because they consist of several quarter-wave length coupled lines which occupy a large area at low frequency bands.

Thus, lumped-type baluns such as planar transformers, lumped 180° hybrid couplers, 180° power splitters, and a lattice-type balun, have been widely applied to the production narrow band microwave integrated circuits because they require smaller areas than the distributed-type ones in low frequency regimes [2-4, 10, 12, 15]. In order to improve their bandwidth and the phase error characteristics, the fifth order low pass filter and high pass filter were utilized by using their compensating structures [3, 4]. Also the second-order lattice-type LC balun was investigated for its wideband operation [15].

However, it is not easy to maintain both a 180° phase difference and an identical magnitude of two balanced ports. These methods require an increase in the number of lumped elements which cause an increase in insertion loss and device size. Furthermore, they do not provide DC isolation characteristics between the unbalanced and balanced ports from the driving power of the RF integrated circuits. In order to reduce the number of lumped elements and enhance the performance of the balun, a coupling method was applied [19]. The micro balun transformer reported here was designed with coupled LC resonators and embedded into a multi-layered PCB (printed circuit board) with a high dielectric $BrTiO_3$ composite film. The coupling method between the adjacent resonators is considered to be a powerful one in the design of RF devices, especially in respect of bandpass filters [20, 21]. It is comprised two pairs of coupled LC resonators which shared one resonator for magnetic coupling. The proposed design obviously provided an identical magnitude and phase difference of 180° between two balanced ports. Furthermore, it also exhibited DC isolation and an impedance transformation characteristic between the un-

† Corresponding Author: Dept. of Electronic Engineering, Kwangwoon University, Seoul, Korea. (jaepark@kw.ac.kr)
* Dept. of Electronic Engineering, Kwangwoon University, Seoul, Korea. (jongcheol.park@kw.ac.kr, ymks21@gmail.com)
Received: April 17, 2014; Accepted: December 13, 2014

balanced and balanced ports.

This paper presented a semi-lumped balun using conventional PCB process and detailed numerical and theoretical analysis of the lumped balun transformer with three pairs of coupled LC resonators. The circuit design and analysis was first performed by transforming the proposed three resonators circuit into an equivalent two resonators circuit by the use of a balanced mode analysis. Through these theoretical analyses, crucial design considerations and parameters were investigated for obtaining a maximally flat response in the pass-band, good phase / magnitude imbalances, and large bandwidth. Finally, the proposed balun circuit was fabricated by using conventional 4-layered PCB process and numerically calculated, EM simulated, and measured performance characteristics were compared and discussed.

2. Design and Fabrication

2.1 Balun transformer circuits

The proposed balun circuit was designed by combining two pairs of magnetically coupled resonators with mutual inductances (M_{21}, M_{31}), as shown in Fig. 1. The left and right side resonators are denoted as the primary and secondary ones, respectively. The inductors (L_{s1} and L_{s2}) of the secondary resonators can be expressed by the impedance transfer ratio ($2N=R_L/R_s$) and the primary inductor (L_p) is given by $L_s=NL_p$. The phase delay of the magnetically coupled LC resonator is strongly dependent on the geometrical configuration of the inductor which is divided by its winding direction such as the same and opposite ones. When the two balanced ports have the same secondary inductances, their voltage and current magnitude can be given as $L_{s1}=L_{s2}$, $v_{s1}=-v_{s2}$, and $i_{s1}=i_{s2}$. Although they obviously have the same magnitude characteristics, their phase delays are opposite to each other. Therefore, the proposed balun circuit was designed to have an identical magnitude and 180 degree phase difference between the two balanced ports. The output voltage between the balanced ports is given as $v_s=v_{s1}-v_{s2}$. Since the currents, i_p and i_s flow in opposite directions, $M=M_{21}=M_{31}$ is always positive. The mutual inductance, M between the primary and secondary inductors can be derived from their self-inductances and coupling coefficient of k.

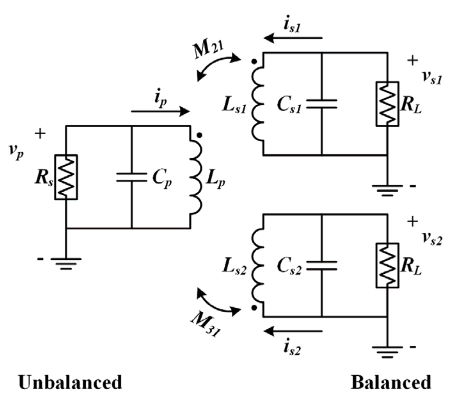

Fig. 1. Schematic diagram of proposed balun transformer with two pairs of coupled LC resonators.

$$M=\sqrt{2}k\sqrt{L_pL_s} \tag{1}$$

The mutual inductance in the proposed balun with three LC resonators has a square root twice as large as that of two port coupled LC resonators. In order to perform extra analysis of the transmission characteristic of the proposed balun circuit, it is simplified as a two ports circuit by connecting two balanced ports and modes as shown in Fig. 2. Fig. 2 (a) shows a two port transformed circuit and an equivalent circuit model of the proposed balun transformer. From (1), the equivalent secondary inductance, L'_s, capacitance, C'_s, effective coupling coefficient, k', can be obtained as $L'_s=2L_s$, $C'_s=C_s/2$, and $k'=k\sqrt{2}$, respectively.

The lumped element equivalent circuit of the two port transformed balun circuit can be expressed as shown in Fig. 2 (b) [22]. It is assumed that a two LC resonator has the same resonant frequency, ω_0. As shown in Fig. 2 (b), it has the reference plane of T-T'. Therefore, the input impedance of the even mode, Z_{ine} and odd mode, Z_{ino} at a single-ended port is given as

$$Z_{ine,ino}=\frac{j\omega L_p\left(1\pm k'\right)}{1-\left(\omega/\omega_0\right)^2\left(1\pm k'\right)} \tag{2}$$

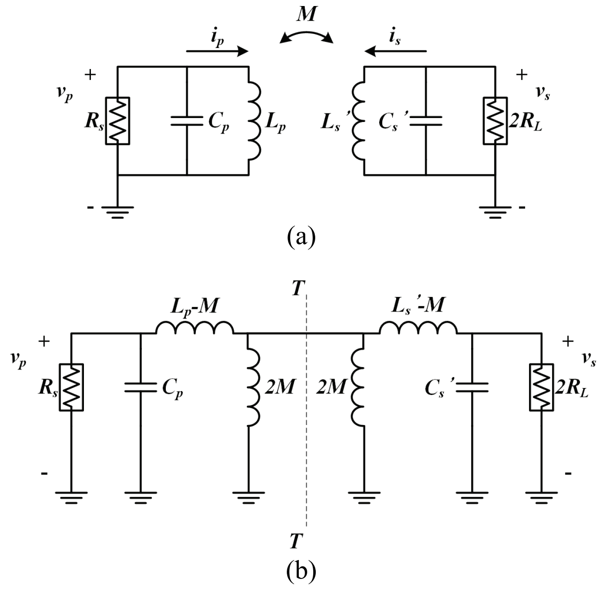

Fig. 2. Equivalent circuit of proposed balun transformer with two pairs of coupled LC resonators: (a) Two port circuit for balanced mode of proposed balun transformer and (b) Equivalent circuit model of transformed two port circuit.

Hence, the input impedance can be described as

$$Z_{in} = \frac{j\left(\omega/\omega_0\right)\sqrt{\frac{L_p}{C_p}}\sqrt{1-k'^2}}{\sqrt{\left(\omega/\omega_0\right)^4\left(1-k'^2\right)-2\left(\omega/\omega_0\right)^2+1}} \qquad (3)$$

where Z_{in} is the input impedance which is derived from $Z_{in} = \sqrt{Z_{ine}Z_{ino}}$.

In the same manner, the output impedance at the balanced port is given by the equation

$$Z_{out} = \frac{j\left(\omega/\omega_0\right)\sqrt{\frac{L'_s}{C'_s}}\sqrt{1-k'^2}}{\sqrt{\left(\omega/\omega_0\right)^4\left(1-k'^2\right)-2\left(\omega/\omega_0\right)^2+1}} \qquad (4)$$

Therefore, the relationship between input and output impedance is described as

$$Z_{out} = 2NZ_{in} \qquad (5)$$

As shown in the above results, the proposed balun circuit behaves as an impedance transformer with a ratio *1*:*2N*. From (3) and (4), the resonant frequency separated by the magnetic coupling is given by the equation

$$\omega_{h,l} = \frac{1}{\sqrt{(1 \mp k')}}\omega_0 \qquad (6)$$

where ω_h and ω_l are the resonant frequencies in the higher and lower frequency region, respectively.

From (2), (3), and (4), the transmission and reflection characteristics shown in Fig. 3 can be explained by the input impedance of proposed balun circuit as shown in Fig. 4. As shown in Figs. 3 and 4, the insertion loss and ripple in the passband are strongly dependent on the input impedance of the balun circuit which is a function of the coupling coefficient. Furthermore, the real part of the input impedance is predominant when the frequencies are around the natural frequency of LC resonator, ω_0. The reduced coupling serves to increase the insertion loss wheras over coupling causes a large ripple in the passband. As shown in Fig. 4, a large insertion loss and ripple are observed when the input impedance is larger or smaller than the source impedance, respectively.

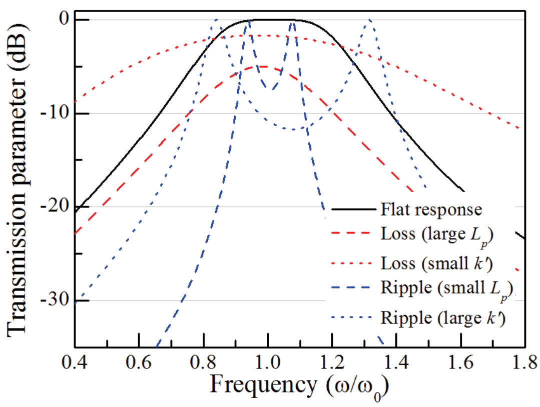

Fig. 3. Calculated transmission characteristics for the maximum flat response in pass band, large insertion loss caused by the large inductance and small coupling coefficient, and large ripple caused by the small inductance and large coupling.

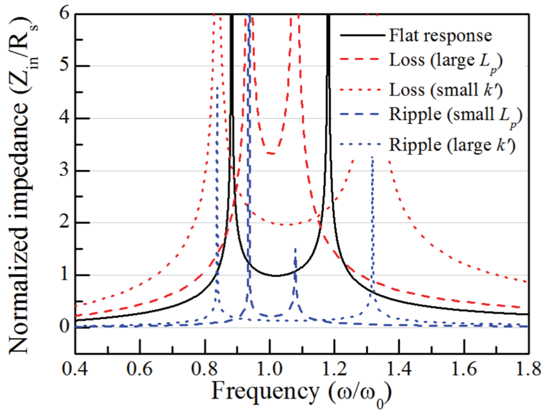

Fig. 4. Calculated input impedance normalized by source impedance of proposed balun circuit with various combination of coupling coefficient and component values for the maximum flat response in pass band, large insertion loss due to large inductance and small coupling coefficient, and large ripple due to small inductance and large coupling.

2.2 Synthesization for maximally flat response in passband

The transmission characteristic is discussed here in order to determine the condition for a maximally flat response in the passband. As shown in Fig. 3 and 4, the maximally flat response is observed when the input impedance, Z_{in}, is matched with the source impedance, R_s. From (3), the input impedance at the natural frequency ($\omega=\omega_0$) can be expressed as

$$Z_{in} = \frac{\omega_0 L_p\sqrt{1-k'^2}}{k'} \qquad (7)$$

In order to obtain the maximally flat response in the passband, the maximum power transfer condition between the source and input of the balun circuit is applied at the natural frequency of the LC resonator(ω_0) as given by $R_s=Z_{in}$.

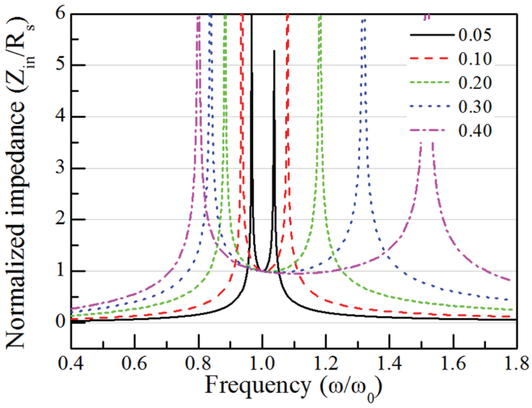

Fig. 5. Calculated and normalized input impedances of proposed balun transformer with various coupling coefficients at the condition of maximally flat response in its passband.

$$L_p = \frac{R_s}{\omega_0}\sqrt{\frac{k'^2}{1-k'^2}} \tag{8}$$

$$C_p = \frac{1}{R_s\omega_0}\sqrt{\frac{1-k'^2}{k'^2}} \tag{9}$$

Fig. 5 shows the calculated input impedance which is normalized by the source impedance R_s from (3), (7), (8), and (9). As shown in Fig. 5, the input impedance is well matched to the source impedance across the passband. Hence, the s-parameter can be derived as a function of k' and frequency, as shown by the equations

$$s_{11} = \frac{-a^4\left(1-k'^2\right)+a^2\left(2-k'^2\right)-1}{a^4\left(1-k'^2\right)-2ja^3k'\sqrt{1-k'^2}-a^2\left(2+k'^2\right)+2ja\frac{k'}{\sqrt{1-k'^2}}+1} \tag{10}$$

$$s_{21} = \frac{ja\frac{2k'^2}{\sqrt{1-k'^2}}}{a^4\left(1-k'^2\right)-2ja^3k'\sqrt{1-k'^2}-a^2\left(2+k'^2\right)+2ja\frac{k'}{\sqrt{1-k'^2}}+1} \tag{11}$$

where a is the ratio of applied frequency and natural frequency of the LC resonator given by $a=\omega/\omega_0$.

From (10), the two resonance poles can be found when a is 1 and $1/\sqrt{1-k'^2}$, as shown in Fig. 6 (b). As the coupling coefficient, k increases, the center frequency also increases slightly as a function of k.

$$\omega_c = \omega_0\frac{\sqrt{1-k'^2}+1}{2\sqrt{1-k'^2}} \tag{12}$$

The bandwidth was determined as the frequency range when the transmission coefficient is over 3 dB. It can be derived from (6) as

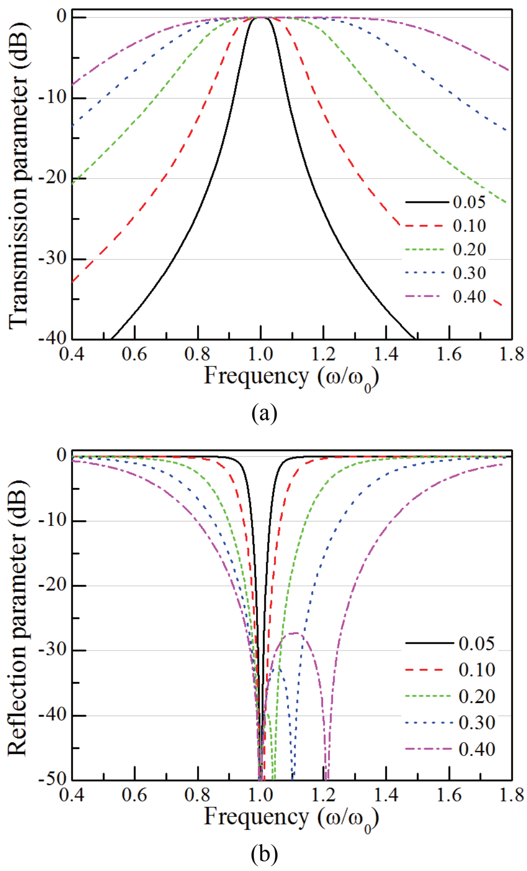

Fig. 6. Calculated s-parameter of proposed balun transformer with various coupling coefficients: (a) Insertion loss and (b) Return loss.

$$BW = \sqrt{2}\omega_0\frac{\sqrt{1+k'}-\sqrt{1-k'}}{\sqrt{1-k'^2}} \tag{13}$$

As shown in Fig. 6, the maximally flat response in the passband can be obtained from the desired center frequency, operating bandwidth, and impedance ratio by using the conditions given by (8) and (9).

3. Experimental Results and Discussions

3.1 Demonstration of the proposed balun transformer

As shown in Fig. 2, there are several design parameters for the proposed balun device such as inductance, capacitance, coupling coefficient, and impedance ratio between the input and output ports. In order to design the device effectively, these parameters must be derived from the following key features:

1) Center frequency (ω_c) and operating bandwidth.
2) Impedance ratio (N) between the source and load.

From equation (12) and (13), the effective coupling coefficient (k') can be defined from the above features such as center frequency and bandwidth. Furthermore, the values of lumped element for proposed balun transformer can be obtained from the effective coupling coefficient (k'), center frequency (ω_c), impedance ratio (N), and designated source and load impedance by using equation (8) and (9). In order to validate the proposed concept of design, the balun circuit was demonstrated by using conventional 4-layered PCB process as shown in Fig 7. Three balun transformers were designed with a center frequency of 500 MHz and an impedance transfer ratio of 50Ω:100Ω. Each device has 3 dB bandwidth of 100 MHz, 210 MHz, and 330 MHz and its corresponding coupling coefficient is 0.1, 0.2 and 0.3, respectively. The desired values of the embedded inductors (L_P=L_S) were calculated from (8) as shown in Table 1. The designated length and gap of embedded inductor was calculated by considering as a conductor with rectangular crosssection [23, 24]. The calculated geometric parameters of embedded inductors were optimized by using 3D EM simulation based DOE (design of experiments) method to embed them into a conventional 4-layered 0.8T PCB substrate. As shown in Fig. 7 (a), the embedded inductors were configured by top and bottom conductor with through hole via and they have a width of 0.5 mm and 0.45 mm for primary (L_p) and secondary (L_s) inductors, respectively. Table 1 presents the geometric parameters and component values of proposed balun based on 0.8T PCB process. The optimized values of the embedded inductors and gap using 3D EM simulation were inductances of 2.6 nH, 5 nH, and 7.9 nH and distances of 0.325 mm, 0.2 mm, and 0.1 mm for the coupling coefficient of 0.1, 0.2, and 0.3, respectively. The standard 0603 sized muRata chip lumped capacitors were employed to configure the LC resonator. Fig. 8 shows top views of the fabricated balun transformer using conventional 4-layered 0.8T PCB and lumped chip capacitors.

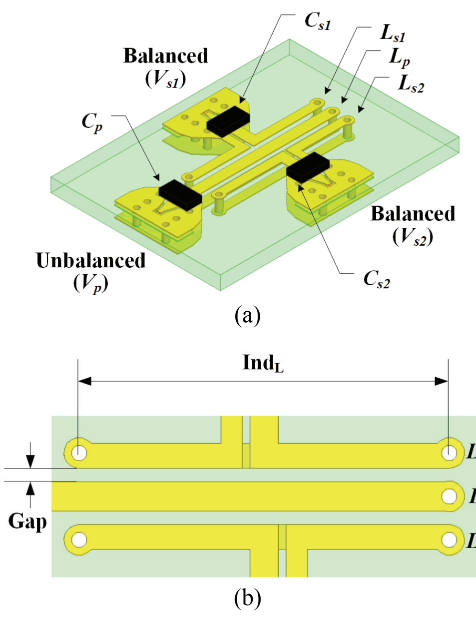

Fig. 7. Schematic drawing of proposed balun transformer using coupled LC resonator: (a) Three-dimensional view of proposed balun transformer based on 4-layered PCB with lumped chip capacitors and (b) Geometrical parameter for PCB embedded inductors and coupling coefficient.

3.2 Measured results and discussions

The fabricated balun transformers have been characterized by the use of an HP E5071C network analyzer after SOLT calibration. PICOPROBE coplanar ground-signal-ground probes with 250 μm in pitch size were used. The measured frequencies were ranged from 0.2 GHz to 0.8 GHz. Fig. 9 shows 3D EM simulated and measured results for the fabricated balun transformers using coupled LC resonator. The solid lines represent the measured results and the dashed lines denote the 3D-EM simulated ones

As shown in Fig. 9, the fabricated balun transformer has slightly narrower bandwidth and larger insertion loss than the theoretically designed device (short dashed line) because it is not easy to control the dimensions required for designated inductances during PCB fabrication. The fabricated primary and secondary inductors on 1st and 4th layer for balun transformer have approximately 25μm and

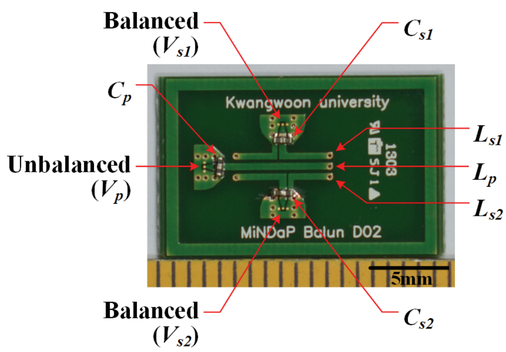

Fig. 8. Photograph of fabricated balun transformer using coupled LC resonator using embedded inductors and lumped chip capacitors based on the conventional 0.8 T 4-layered PCB process.

Table 1. Calculated geometric parameters for PCB embedded inductor and capacitance value of proposed balun transformer.

Device	Bandwidth (MHz)	Coupling coefficient (k)	Gap (mm)	L_p (nH)	Ind$_L$ (mm)	Width (mm)		C_p (pF)	Area (mm^2)
						L_p	L_s		
D01	100	0.1	0.325	2.25	2.4	0.5	0.45	44	4.2 ×3.1
D02	210	0.2	0.200	4.7	6.1	0.5	0.45	22	7.9×2.9
D03	330	0.3	0.100	7.5	10.5	0.5	0.45	13.6	12.3 ×2.7

Table 2. Summary of measured results of fabricated three balun transformer to have bandwidth of 100 MHz (D01), 210 MHz (D02), and 330 MHz (D03) and center frequency of 500 MHz.

Device	3dB bandwidth (MHz)	Insertion loss (dB)			Return loss (dB, Max)	Magnitude difference (dB, Max)	Phase difference (degree, Max)
		Frequency (MHz)	Balance (Max)	Common (Min)			
D01	414 ~ 525	435 ~ 467	3.15	28.7	7.6	0.36	0.65
D02	378 ~ 569	419 ~ 534	1.48	27.7	10	0.78	2
D03	336 ~ 632	414 ~ 579	1.64	28.9	10	0.8	2.4

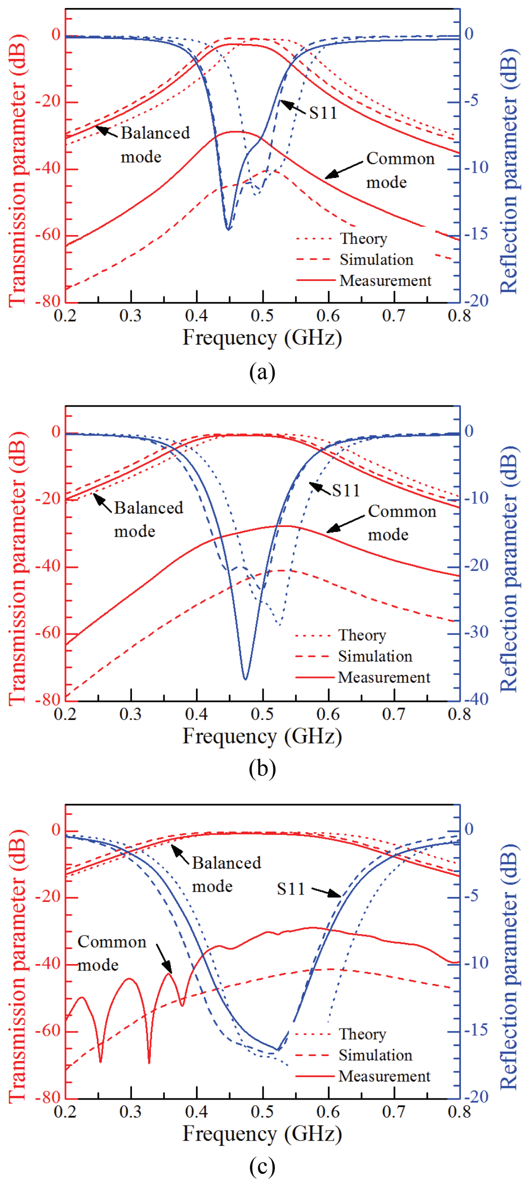

Fig. 9. Measured and 3D EM simulated frequency responses of three fabricated balun transformers based on conventional 0.8T 4-layered PCB process: (a) Balun transformer with bandwidth of 100 MHz (D01), (b) Balun transformer with bandwidth of 210 MHz (D02), and (c) Balun transformer with bandwidth of 330 MHz (D03).

50μm smaller width than the designated ones, respectively. Furthermore, the total thickness of fabricated PCB has approximately 150μm thicker than the designated one.

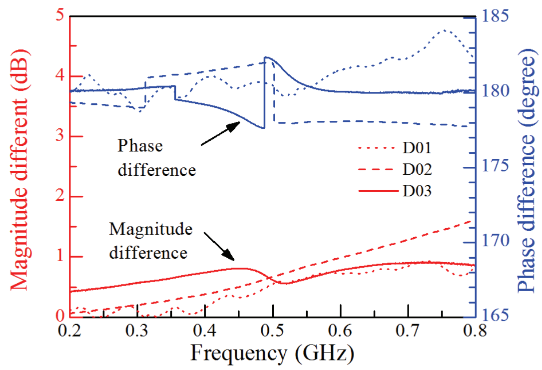

Fig. 10. Measured phase and magnitude imbalance characteristic of three fabricated balun transformers to have bandwidth of 100 MHz (D01), 210 MHz (D02), and 330 MHz (D03)

These resulted in the increase of inductance and the decrease of coupling coefficient. Therefore, the resonant frequency of fabricated balun transformer was slightly shifted to lower frequency as shown Fig. 9. The simulation results (dashed line) in Fig. 9 represent the 3D EM simulated ones of the fabricated balun device by using the measured geometrical parameters. They were well matched with the measured ones. Therefore, the proposed design theory and geometry of balun transformer is highly useful by keeping the fabrication tolerance of PCB. Table 2 shows the summary of measured results of fabricated balun transformer. The fabricated balun device exhibited good phase and magnitude imbalance characteristics with sufficiently large bandwidth as shown in Fig. 10. Furthermore, it has DC isolation characteristics between the unbalanced and balanced ports.

4. Conclusion

A semi-lumped balun transformer based on coupled LC resonators has been designed, fabricated, and characterized by using conventional 4-layered PCB process. The theoretical analysis based on balanced mode was performed to find the optimal design parameters for wideband frequency responses with low insertion loss and ripple. The proposed balun transformer was synthesized and demonstrated by using planar inductors embedded into conventional 4-layered 0.8T PCB substrate and standard 0604 sized chip capacitors to verify the derived theory. It showed a good phase and magnitude imbalance characteristic, and DC isolation characteristics between the unbalanced and balanced ports with impedance trans-formation.

Acknowledgements

This research was supported by the Pioneer Research Center Program (2010-0019313) and Basic Science Research Program (NRF-2013R1A1A2A10064810) through the National Research Foundation of Korea funded by the Ministry of Education, Science and Technology. The authors are grateful to MiNDaP group members for their technical support and discussions.

References

[1] N. Marchand, "Transmission-line conversion transformers," *Electron,* vol. 17, pp. 142-146, 1944.

[2] S. J. Parisi, "180 degrees lumped element hybrid," in *Microwave Symposium Digest, 1989., IEEE MTT-S International*, 1989, pp. 1243-1246.

[3] H.-K. Chiou and H.-H. Lin, "A miniature MMIC double doubly balanced mixer using lumped dual balun for high dynamic receiver application," *Microwave and Guided Wave Letters, IEEE,* vol. 7, pp. 227-228, 1997.

[4] H.-K. Chiou, H.-H. Lin, and C.-Y. Chang, "Lumped-element compensated high / low-pass balun design for MMIC double-balanced mixer," *Microwave and Guided Wave Letters, IEEE,* vol. 7, pp. 248-250, 1997.

[5] S. Lee, "A Novel CPW Balanced Distributed Amplifier Using Broadband Impedance-Transforming MEMS Baluns," *Journal of Electrical Engineering & Technology,* vol. 8, p. 3, 2013.

[6] S. Kahng, J. Lee, K.-T. Kim, and H.-S. Kim, "Metamaterial CRLH Structure-based Balun for Common-Mode Current Indicator," *Journal of Electrical Engineering & Technology,* vol. 9, pp. 301-306, 2014.

[7] Y. Fujiki, H. Mandai, and T. Morikawa, "Chip type spiral broadside coupled directional couplers and baluns using low temperature co-fired ceramic," in *Electronic Components and Technology Conference, 1999. 1999 Proceedings. 49th*, 1999, pp. 105-110.

[8] K. Nishikawa, I. Toyoda, and T. Tokumitsu, "Compact and broad-band three-dimensional MMIC balun," *Microwave Theory and Techniques, IEEE Transactions on,* vol. 47, pp. 96-98, 1999.

[9] Y. J. Yoon, Y. Lu, R. C. Frye, M. Y. Lau, P. R. Smith, L. Ahlquist*, et al.*, "Design and characterization of multilayer spiral transmission-line baluns," *Microwave Theory and Techniques, IEEE Transactions on,* vol. 47, pp. 1841-1847, 1999.

[10] J. R. Long, "Monolithic transformers for silicon RF IC design," *Solid-State Circuits, IEEE Journal of,* vol. 35, pp. 1368-1382, 2000.

[11] C.-W. Tang, J.-W. Sheen, and C.-Y. Chang, "Chip-type LTCC-MLC baluns using the stepped impedance method," *Microwave Theory and Techniques, IEEE Transactions on,* vol. 49, pp. 2342-2349, 2001.

[12] W. Bakalski, W. Simburger, H. Knapp, H.-D. Wohlmuth, and A. L. Scholtz, "Lumped and distributed lattice-type LC-baluns," in *Microwave Symposium Digest, 2002 IEEE MTT-S International*, 2002, pp. 209-212.

[13] C.-W. Tang and C.-Y. Chang, "A semi-lumped balun fabricated by low temperature co-fired ceramic," in *Microwave Symposium Digest, 2002 IEEE MTT-S International*, 2002, pp. 2201-2204.

[14] Y.-J. Ko, J. Y. Park, J.-H. Ryu, K.-H. Lee, and J. U. Bu, "A miniaturized LTCC multi-layered front-end module for dual band WLAN (802.11 a/b/g) applications," in *Microwave Symposium Digest, 2004 IEEE MTT-S International*, 2004, pp. 563-566.

[15] D. Kuylenstierna and P. Linnér, "Design of broad-band lumped-element baluns with inherent impedance transformation," *Microwave Theory and Techniques, IEEE Transactions on,* vol. 52, pp. 2739-2745, 2004.

[16] D. Staiculescu, N. Bushyager, A. Obatoyinbo, L. J. Martin, and M. M. Tentzeris, "Design and optimization of 3-D compact stripline and microstrip Bluetooth / WLAN balun architectures using the design of experiments technique," *Antennas and Propagation, IEEE Transactions on,* vol. 53, pp. 1805-1812, 2005.

[17] B. H. Lee, D. S. Park, S. S. Park, and M. C. Park, "Design of new three-line balun and its implementation using multilayer configuration," *Microwave Theory and Techniques, IEEE Transactions on,* vol. 54, pp. 1405-1414, 2006.

[18] C. Cho and K. Gupta, "A new design procedure for single-layer and two-layer three-line baluns," *Microwave Theory and Techniques, IEEE Transactions on,* vol. 46, pp. 2514-2519, 1998.

[19] J. Park and J. Y. Park, "FR-4 Embedded Wideband Micro-Balun with Coupled LC Resonators," in *Microwave Conference, 2008. EuMC 2008. 38th European*, 2008, pp. 333-336.

[20] J.-S. Hong, "Couplings of asynchronously tuned coupled microwave resonators," *IEE Proceedings-Microwaves, Antennas and Propagation,* vol. 147, pp. 354-358, 2000.

[21] W. -S. Tung, Y. -C. Chiang, and J. -C. Cheng, "A new compact LTCC bandpass filter using negative coupling," *Microwave and Wireless Components Letters, IEEE,* vol. 15, pp. 641-643, 2005.

[22] J.-S. G. Hong and M. J. Lancaster, *Microstrip filters for RF/microwave applications* vol. 167: John Wiley & Sons, 2004.

[23] E. B. Rosa, *The self and mutual inductances of linear conductors*: US Department of Commerce and Labor, Bureau of Standards, 1908.

[24] F.W. Grover, *Inductance calculations: working formulas and tables*: Courier Dover Publications, 2004.

Jongcheol Park He received his M.S. and Ph.D. degrees in Electronic Engineering from Kwangwoon University, Seoul, Korea in 2009 and 2013, respectively. He worked as a BK postdoc at same institute about one year from graduation. Then he joined as a project researcher in National Nano Fab Center, Korea, since Dec. 2014. His research focuses on various fields of MEMS devices, such as energy harvesting, optical, RF passives and flexible electronics.

Minkyu Yoon He received B.S. and M.S. degrees in the Dept. of Electronic Engineering from Kwangwoon University, Seoul, Korea, in 2012 and 2014, respectively. He is currently working at Research and Develop in Samsung Electronics Co., Ltd. His research focuses on various MEMS actuators, such as electro static MEMS switches, tunable devices and RF passive devices.

Jae Yeong Park He received his Ph.D. degree in electrical and computer engineering from Georgia Institute of Technology, Atlanta, in 1997. After graduation, he worked as a research scientist at the same institution for more than one year. Then he joined as a Senior Research Engineer in LG Electronic Institute of Technology, Korea in 1999 and promoted as Chief Research Engineer in 2001. In September 2004, he joined as an Assistant Professor in the Department of Electronic Engineering of Kwangwoon University, Korea and presently he is working as a Professor. He has contributed to more than 200 international conference papers and peer-reviewed journal articles in the fields of piezoelectric MEMS sensors and actuators, Optical MEMS, RF MEMS, Bio-sensors, and Energy harvesting. He is holding more than 110 patents on his name. He is also a reviewer and an editor of a number of renowned journals in the fields mentioned above. His current research interests include MEMS energy-harvesting devices and systems, piezoelectric and electrostatic micro-actuators for optical and RF applications, electrochemical biosensors and storage devices, and embedded passive devices and chip technology.